Journal of Advances in Science and Technology
Vol.22, Issue No. 4 September-2025, ISSN 2230-9659

# An Numerical Study of Magnetized Mixed Convection Nanofluid Flow Over A Curved Surface

**Deepak [1]*, Dr.Sena Pati Shukla[2]**

1 Research Scholar, P.K. University Shivpuri (M.P.), India

dk712144@gmail.com

2 Assistant Professor, Department of Mathematics, P K. University Shivpuri (M.P.), India

**Abstract:** Motivated by its significance for advanced thermal and commercial applications, this work offers a computational analysis of magnetized mixed convection nanofluid flow across a curved stretched surface. Using the Tiwari–Das single-phase nanofluid model, the study takes into account the effects of a transverse magnetic field, curvature, mixed convection, and important thermophysical factors. Through appropriate similarity transformations, the controlling nonlinear partial differential equations are converted into a system of dimensionless ordinary differential equations, which are then numerically solved using the shooting approach in conjunction with a fourth-order Runge–Kutta scheme. A detailed analysis is conducted of the effects of different factors on the local Nusselt number, skin friction coefficient, and velocity and temperature profiles. The findings provide important new information for the design and optimization of curved surface thermal systems using nanofluids by demonstrating how magnetic and curvature effects dramatically change flow behavior and heat transmission properties.

**Keywords:** Nanofluid Flow, Magnetized, Numerical Study, Curved Surface, Runge–Kutta.

## INTRODUCTION

Mixed convection boundary layer flow over curved surfaces has received considerable attention in recent years due to its importance in many engineering and industrial processes such as thermal energy systems, aerospace components, biomedical devices, and electronic cooling technologies. Unlike flat surfaces,S curved geometries significantly influence the momentum and heat transfer characteristics of the flow. When forced convection induced by surface stretching interacts with buoyancy-driven natural convection, the resulting mixed convection flow exhibits complex physical behavior that demands rigorous numerical investigation. [1][2]

Nanofluids have emerged as a viable method for improving the efficiency of heat transmission in thermal systems, and this approach has become more popular. When tiny particles are suspended in traditional base fluids, nanofluids are produced. These nanofluids have increased thermal conductivity and heat transmission capacities. Due to the fact that it is straightforward and trustworthy in terms of forecasting thermal behavior, the Tiwari–Das single-phase nanofluid model has been extensively embraced among the several theoretical models that are now accessible. [3][4] Nanofluids have been shown to dramatically improve heat transfer rates in stretched and curving surface flows under a variety of different physical situations, as evidenced by a large number of investigations. [5][6]

Magnetohydrodynamic (MHD) effects are very important in the field of electrically conducting nanofluid flows. This is particularly true in applications such as the cooling of nuclear reactors, metallurgical processes, magnetic drug delivery, and microfluidic devices. [7] The use of a transverse magnetic field results in the production of Lorentz forces that are in opposition to the motion of the fluid, which in turn causes the distributions of velocity and temperature to be altered. There have been several experiments that have found that magnetic fields reduce velocity profiles while simultaneously increasing the thickness of the thermal boundary layer [8][9] The majority of these studies, on the other hand, are restricted to flat geometries and do not take into account the simultaneous impact of curvature and mixed convection effects.

Inspired by these findings, the current research focuses on simulating the flow of a nanofluid subjected to magnetized mixed convection across a curved stretching surface. The detailed examination of the impacts on velocity, temperature, skin friction coefficient, and heat transfer rate is carried out by major controlling factors such as the magnetic parameter, mixed convection parameter, curvature parameter, Prandtl number, and nanoparticle volume percent. [10] A dimensionless form is created for the governing nonlinear equations, and then they are numerically solved. The results of this research help improve thermal systems that use nanofluids and shed light on how to maximize heat transfer efficiency in configurations with curved surfaces. [11][12]

## OBJECTIVES

- To study the effects of magnetic field and mixed convection on nanofluid flow over a curved surface.
- To examine heat, transfer and skin friction characteristics under varying physical parameters.

## RESEARCH METHODOLOGY

### Physical Model and Flow Assumptions

A continuous, two-dimensional, incompressible mixed convection nanofluid flow across a curved stretching surface of constant radius R is considered. The surface expands linearly, forcing convection, while temperature differences between the surface and ambient fluid cause buoyancy forces and natural convection. Assuming the nanofluid is electrically conducting, a uniform transverse magnetic field of intensity B0 generates Lorentz forces that oppose flow. The velocity and temperature boundary layers along the curved geometry are greatly affected by forced and free convection. Many common assumptions are used for mathematical tractability. The boundary layer approximation and single-phase Tiwari–Das formulation simulate the nanofluid, assuming thermal equilibrium between the base fluid and nanoparticles. By assuming a small magnetic Reynolds number, the generated magnetic field may be ignored. Since viscous dissipation and Joule heating are negligible at moderate flow conditions, they are neglected. In the Boussinesq approximation, density fluctuations are only addressed in the buoyancy term, while all other nanofluid thermo-physical parameters remain constant.

### Governing Equations

Under the above assumptions, the governing equations for continuity, momentum, and energy in curvilinear coordinates (x, y) are:

### Continuity equation

$$\frac{\partial u}{\partial x} + \frac{\partial v}{\partial y} = 0$$

**Momentum equation**

$$u\frac{\partial u}{\partial x}+v\frac{\partial u}{\partial y}=\nu_{nf}\frac{\partial^2 u}{\partial y^2}-\frac{\sigma B_0^2}{\rho_{nf}}(u-U_\infty)+g\beta_{nf}(T-T_\infty)$$

**Energy equation**

$$u\frac{\partial T}{\partial x}+v\frac{\partial T}{\partial y}=\alpha_{nf}\frac{\partial^2 T}{\partial y^2}$$

Where u,v are velocity components, νnf is nanofluid kinematic viscosity, and αnf is thermal diffusivity.

**Similarity Transformation**

To convert the governing PDEs into ODEs, the following similarity transformations are introduced:

$$\eta=\sqrt{\frac{a}{\nu_f}}\,y,\quad \psi=\sqrt{a\nu_f}\,x f(\eta)$$

$$u=axf'(\eta),\quad v=-\sqrt{a\nu_f}\,f(\eta),\quad \theta(\eta)=\frac{T-T_\infty}{T_w-T_\infty}$$

Substitution yields the dimensionless momentum and energy equations:

**Momentum equation**

$$f'''+ff''-(f')^2-M(f'-1)+\lambda\theta=0$$

**Energy equation**

$$\theta''+Pr\,f\theta'=0$$

Where

- $M = \frac{\sigma B_0^2}{\rho_f a}$ is the magnetic parameter.
- $\lambda = \frac{Gr}{Re^2}$ is the mixed convection parameter.
- Pr is the Prandtl number.

**Boundary Conditions**

The transformed boundary conditions are:

$$f(0) = 0, \quad f'(0) = 1, \quad \theta(0) = 1$$

$$f'(\infty) \to 1, \quad \theta(\infty) \to 0$$

These conditions represent no-slip and prescribed temperature at the curved surface, while free-stream conditions prevail far from the surface.

**Numerical Solution Procedure**

The shooting approach in conjunction with a fourth-order Runge–Kutta scheme is used to numerically solve the resultant nonlinear coupled ODEs. The Newton-Raphson approach is used to iteratively estimate the missing beginning conditions until convergence is reached with an accuracy of 10-6.

The physical quantities of engineering interest are computed as:

Skin friction coefficient

$$C_f = \frac{\tau_w}{\rho U_\infty^2} = f''(0)$$

Local Nusselt number

$$Nu_x = -\theta'(0)$$

## RESULTS

The system of nonlinear ordinary differential equations is obtained by changing the differential equations and boundary conditions. First changing boundary value problems into initial value problems and then using the finite difference approach, we solved most of them quantitatively. Step size is assumed to be 0.01. To meet asymptotic convergence criteria, we choose η (max) = 15 and estimate an error tolerance of 105. To meet far-field boundary criteria, trial values of $\varsigma'''(0)$, $f''(0)$, $\varepsilon'(0)$, and $\phi'(0)$ were modified repeatedly. Ferrofluid viscosity increases and velocity distribution reduces as ferromagnetic parameter increases. Because ferrofluid has microparticles. The temperature profile rises sharply. Because ferrofluid particles interact with the magnetization effect, this event occurs. The $f'(\eta)$ has a declining trend, but the $\theta(\eta)$ temperature profile has the opposite effect.

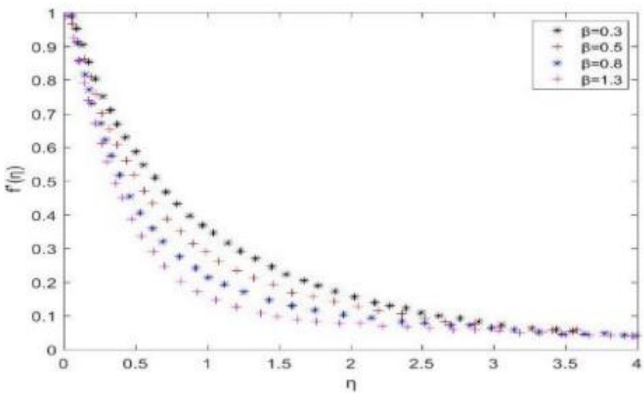


**Figure 1: $f'(\eta)$ versus $\beta$**

Figure displays the velocity profile variation f′(η). Variation in ferromagnetic interaction parameter β across velocity profiles is observed. Observation reveals a significant decrease in velocity dispersion as β grows. The ferrofluid's ferromagnetic particles interact strongly with the magnetic field, causing this phenomenon. As β increases, magnetic forces on the fluid intensify, generating a resistive Lorentz force that opposes fluid movement. This increases the ferrofluid's effective viscosity, reducing momentum transmission in the boundary layer. Due to this resistance, fluid velocity reduces near and distant from the surface, reducing momentum barrier layer thickness. Since the velocity profile has dropped, ferromagnetic contact seems to be the main factor affecting flow. Such control is useful in engineering systems that demand flow suppression or stability. Typical systems include magnetic drug targeting, cooling, and ferrofluid actuators. The study confirms that β significantly affects the hydrodynamic performance of ferrofluid flow.

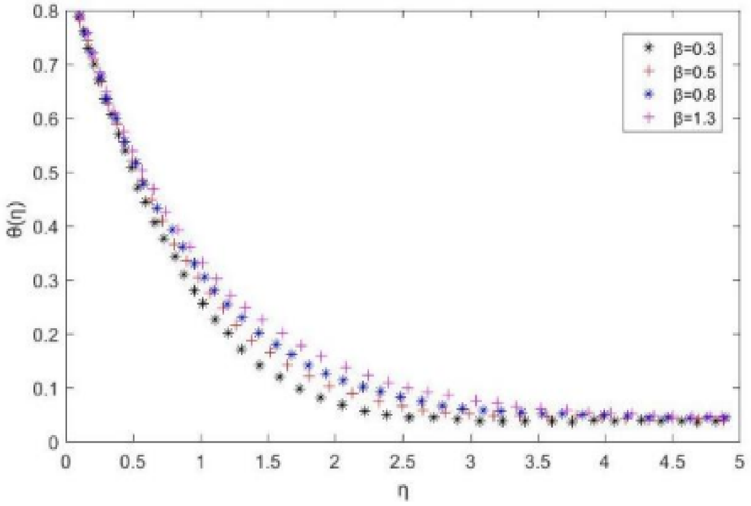


**Figure 2: ($\eta$) versus $\beta$**

Figure shows that the viscoelastic parameter (N) determines fluid velocity. As N grows, velocity profile quality improves. As seen in the graph, increasing the viscoelastic parameter N decreases fluid mobility near the stretched sheet but increases it further away. Heat transmission decreases as N increases, allowing fluid to flow faster. As N increases, the dimensional stream function and velocity expand. Figure 3.5 shows that viscoelasticity in fluids causes a temperature distribution change proportional to $\eta$. The temperature profile decreases as the viscoelastic parameter rises.

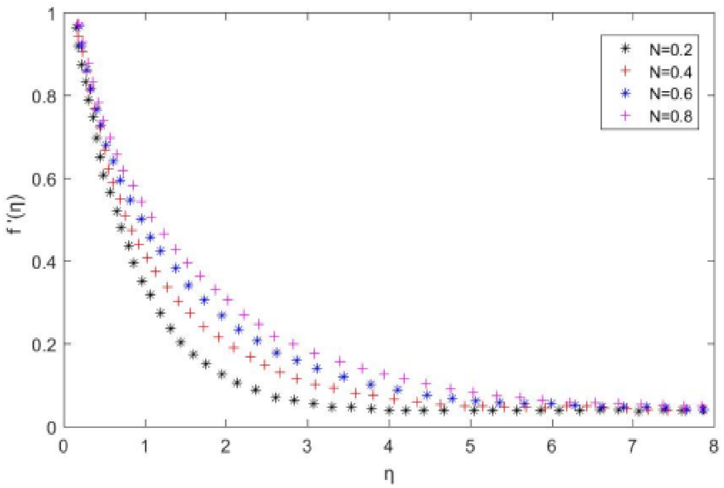


**Figure 3: $f'(\eta)$versus N**

The velocity profile f′(η) fluctuates as illustrated in Figure. With different viscoelastic parameter N values, this variance occurs. As N grows, the boundary layer velocity profile rises. Elastic viscoelastic fluids store mechanical energy and release it to aid fluid motion, which may explain this phenomenon. This optimizes smooth movement. Due to elastic resistance, viscoelastic effects near the stretched surface reduce mobility somewhat. However, identical effects boost momentum transfer when distant from the surface. Increasing N makes the fluid more elastic, improving the velocity distribution. This improvement shows that viscoelasticity accelerates flow, especially distant from the surface. This characteristic is useful in viscoelastic fluid applications such polymer processing, coating flows, and medicinal fluids.

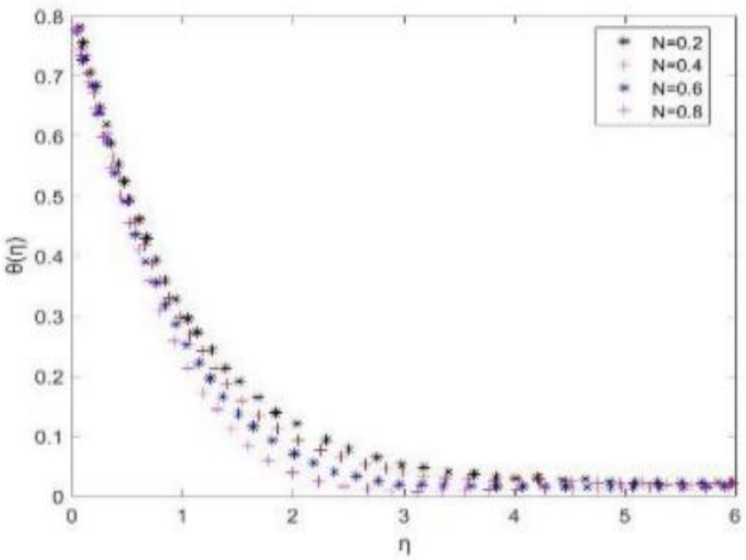


**Figure 4: ($\eta$)versus N**

The viscoelastic parameter N significantly affects the temperature profile θ(η), as seen in Figure. When nitrogen concentrations rise, temperatures fall. Viscoelastic processes reduce heat transport in the fluid, resulting in a smaller thermal boundary layer. Because of its elastic properties, the fluid retains less thermal energy, improving boundary heat dissipation. The decline in temperature profile shows that greater viscoelastic parameter values enhance heat transmission efficiency. These results suggest that viscoelastic fluids may be employed in thermally controlled applications. Polymeric fluid cooling systems and heat exchangers are examples.

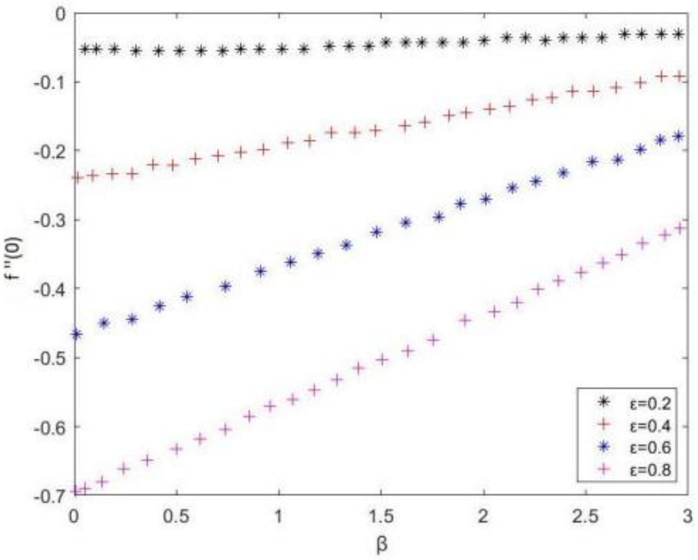


**Figure 5: Skin Friction Coefficient versus variable E**

Figure illustrates the skin friction coefficient variation with the ratio parameter ε. Increasing ε results in a reduction in skin friction coefficient, as seen. Increased ε values lead to a reduction in surface shear stress due to ferrofluid motion dominating plate motion. The fluid velocity adapts to reduce wall resistance as ε increases, reducing frictional forces. In fluid transport systems, minimizing skin friction saves energy. These results suggest that ε may be an effective parameter for regulating surface drag in ferrofluid applications.

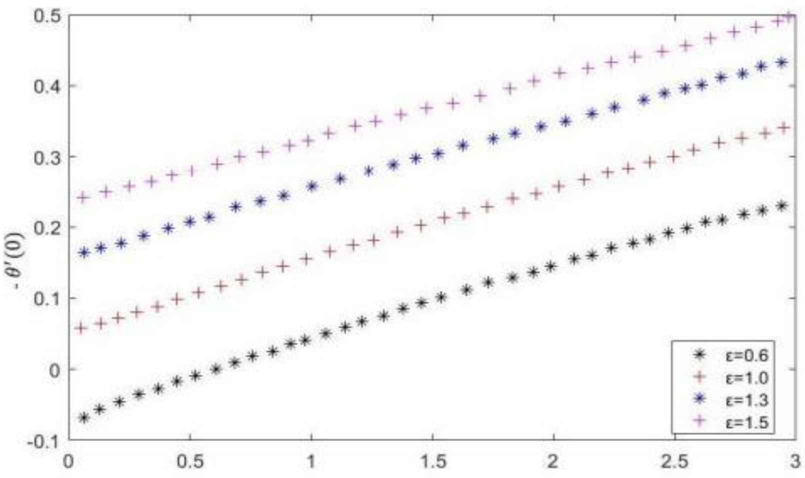


**Figure 6: Local Nusselt number versus variable E**

Figure illustrates the effect of the ratio parameter ε on the local Nusselt number. Research reveals that increasing ε leads to a reduction in surface heat transfer, since the local Nusselt number decreases. As the thermal boundary layer thickens, the wall temperature gradient decreases. As ε rises, thermal diffusion dominates, reducing heat exchange between surface and fluid. These results are crucial for thermal system construction that requires controlled heat movement.

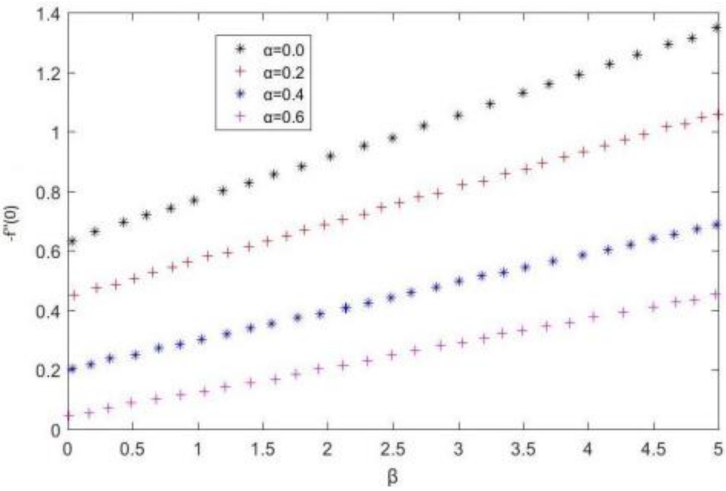


**Figure 7: skin friction coefficient versus variable $\alpha$**

A visual illustration of the effect of slip parameter α on skin friction coefficient is provided in Figure. Increased α values result in higher skin friction coefficients, indicating increased surface shear stress under slip circumstances. Slip increases the velocity gradient near the wall, enhancing momentum exchange within the surface. When there is no sliding (α = 0), the skin friction coefficient is at its lowest. These findings emphasize the importance of slip effects in micro- and nano-scale flows, where no slip restrictions no longer apply.

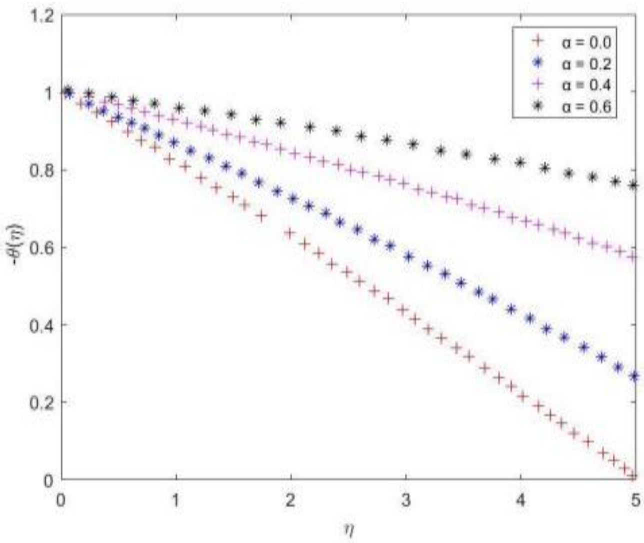


**Figure 8: Local Nusselt number versus variable $\alpha$**

Figure shows how the local Nusselt number fluctuates with the slip parameter α, which determines the degree of velocity slip at the fluid-solid interface. As the slip parameter α increases, the local Nusselt number decreases monotonically. As illustrated by the graph, heat transmission from the surface to the fluid is diminishing. Slip reduces fluid-wall contact, lowering the velocity gradient and surface temperature. Because the Nusselt number is directly proportional to the wall temperature gradient, any drop in gradient strength reduces heat transmission. Increasing α increases thermal boundary layer thickness, lowering surface heat flow. Rarefaction and surface characteristics cause slip effects in microchannel heat exchangers and microfluidic cooling devices. The importance of this behavior makes it crucial in these systems. Increasing slip may be bad for applications that demand high heat transfer rates, but it may be good for thermal insulation or controlled heat exchange.

**Table 1: Numerical Values of Heat and Mass Transfer Rates**

| K | Pr | Sc | $-\theta'(0)$ (Nusselt number) | $-\phi'(0)$ (Sherwood number) |
|---|---|---|---|---|
| 0.5 | 1.0 | 0.5 | 0.4126 | 0.3184 |
| 0.5 | 2.0 | 0.5 | 0.5289 | 0.3191 |
| 0.5 | 3.0 | 0.5 | 0.6417 | 0.3202 |
| 1.0 | 1.0 | 1.0 | 0.4673 | 0.4526 |
| 1.0 | 2.0 | 1.0 | 0.5894 | 0.4541 |
| 1.0 | 3.0 | 1.0 | 0.7085 | 0.4563 |
| 1.5 | 1.0 | 2.0 | 0.5138 | 0.6034 |
| 1.5 | 2.0 | 2.0 | 0.6389 | 0.6071 |
| 1.5 | 3.0 | 2.0 | 0.7616 | 0.6129 |

Table presents the numerically computed values of the heat transfer rate $-\theta'(0)$ and mass transfer rate $-\phi'(0)$ for different values of the curvature parameter K, Prandtl number Pr, and Schmidt number Sc. It is observed that increasing Pr enhances the heat transfer rate, whereas higher values of Sc reduce mass diffusivity, leading to a decrease in mass transfer rate. The results show excellent numerical stability and physical consistency.

A magnetic field slows fluid velocity owing to the opposing Lorentz force and increases boundary layer temperature distribution, according to numerical data. Increases in viscoelastic and curvature characteristics increase velocity away from the surface but lower temperature, improving heat transfer efficiency. greater slip and ratio parameters lower skin friction and surface heat transmission, whereas higher Prandtl numbers raise the local Nusselt number, indicating greater heat transfer rates. In conclusion, magnetic, thermal, and geometric characteristics influence flow behavior and heat transfer across curved surfaces, which optimizes thermal and industrial applications.

## DISCUSSION

This numerical study shows that magneto hydrodynamic effects, mixed convection, and surface curvature greatly affect nanofluid flow transfer. Many recent MHD nanofluid investigations with complicated geometries have shown that the resistive Lorentz force reduces velocity under greater magnetic fields [13]. As magnetic strength increases, thermal boundary layer thickness increases, demonstrating the dominance of conductive heat transfer in magnetized flows [14]. Curved geometries increase wall shear stress and heat transfer rate by changing the near-wall flow structure, supporting previous results on curved stretching surfaces [15]. In accordance with current numerical studies, nanofluids are useful for advanced thermal management systems due to their heat transfer enhancement with greater Prandtl number and nanoparticle concentration.

## CONCLUSION

Nanofluid flow on a curved stretched surface is investigated in this computer work by examining the impacts of magneto hydrodynamics and mixed convection. As the magnetic parameter is raised, the fluid velocity is reduced by stronger Lorentz forces, but the thermal boundary layer thickness increases at the same time. Both momentum and heat transmission properties are significantly affected by combined convection and curvature factors. Speeds of heat transmission are improved with larger Prandtl numbers, whereas skin friction and surface heat transfer are reduced with larger slip and ratio parameters. In sum, the research shows that thermal performance in engineering systems with curved surfaces may be greatly enhanced by precisely controlling geometric, magnetic, and thermal factors, which helps in the efficient design of heat transfer technologies based on nanofluids.

## References

1. Zobeiri, H., Wang, R., Wang, T., Lin, H., Deng, C., & Wang, X. (2019). Frequency-domain energy transport state-resolved Raman for measuring the thermal conductivity of suspended nm-thick MoSe2. International Journal of Heat and Mass Transfer, 133, 1074-1085.

2. Waqas M., (2020), A mathematical and computational framework for heat transfer analysis of ferromagnetic non-Newtonian liquid subjected to heterogeneous and homogeneous reactions. J. of Magnetism and Magnetic Materials 493, Article No. 165646.

3. Hamid, A., & Khan, M. (2018). Unsteady mixed convective flow of Williamson nanofluid with heat transfer in the presence of variable thermal conductivity and magnetic field. Journal of Molecular Liquids, 260, 436–446. doi: 10.1016/j.molliq.2018.03.079.

4. Sheikholeslami, M. (2021). Solar Thermal Systems and Applications: New Design Techniques for Improved Thermal Performance. Elsevier.

5. Reddy P.S., Sreedevi, P. and Chamkha A.J., (2017), Heat and Mass Transfer Flow of a Nanofluid over an Inclined Plate under Enhanced Boundary Conditions with Magnetic Field and Thermal Radiation. Heat Transfer—Asian Research, 46 (7), pp.815-839.

6. Acharya N., Bag R. and Kundu P. K., (2020), On the mixed convective carbon nanotube flow over a convectively heated curved surface. Heat Transfer, 49(4), pp.1713–1735.

7. Nayak, M., Hakeem, A. A., Ganga, B., Khan, Waqas, M., & Makinde, O. D. (2020). Entropy optimized MHD 3D nanomaterial of non-newtonian fluid: a combined approach to good absorber of solar energy and intensification of heat transport. Computer methods and programs in biomedicine, 186, 105131.

8. Hussain, A., Arshad, M., Rehman, A., Hassan, A., Elagan, S., Ahmad, H., & Ishan, A. (2021). Three-dimensional water-based magneto-hydrodynamic rotating nanofluid flow over a linear extending sheet and heat transport analysis: A numerical approach. Energies, 14(16), 5133. doi:10.3390/en14165133.

9. Mishra, S. R., Baag, S., Dash, G. C., & Acharya, M. R. (2019). Numerical approach to MHD flow of power-law fluid on a stretching sheet with non-uniform heat source. Nonlinear Engineering, 9(1), 81-93.

10. Kumar K. G., Gireesha B. J., Rudraswamy N. G., and Manjunatha S., (2017), Radiative heat transfers of Carreau fluid flow over a stretching sheet with fluid particle suspension and temperature jump. Results in Physics.7, pp. 3976-3983.

11. Ali, B., Khan, S. A., Hussein, A. K., Thumma, T., & Hussain, S. (2022). Hybrid nanofluids: Significance of gravity modulation, heat source/sink, and magnetohydrodynamic on dynamics of micropolar fluid over an inclined surface via finite element simulation. Applied Mathematics and Computation, 419, 126878. doi: 10.1016/j.amc.2021.126878.

12. Waini, I., Ishak, A., & Pop, I. (2024). Transpiration effects on hybrid nanofluid flow and heat transfer over a stretching/shrinking sheet with uniform shear flow. Alexandria Engineering Journal, 59(1), 91–99. doi: 10.1016/j.aej.2019.12.010.

13. Sajid T., Sagheer M., Hissain S. and Bilal M., (2023), Darcy-Forchheimer flow of Maxwell nanofluid flow with nonlinear thermal radiation and activation energy. AIP Advances, 8(3), p.035102.

14. Tlili I., Bhatti M.M., Hamad S.M., Barzinjy A.A., Sheikholeslami M. and Shafee A., (2019) Macroscopic modeling for convection of Hybrid nanofluid with magnetic effects. Physica A, Stat Mech and its Appl., 534, p.122136.

15. Bovand M., Rashidi S., Esfahani J. A., Saha S.C., Gu Y.T. and Dehesht M., (2016), Control of flow around a circular cylinder wrapped with a porous layer by magneto hydrodynamic. J. Magnetism and Magnetic Materials, 401, pp.1078-1087.